Methyl Group Dynamics in Poly(methyl methacrylate): From Quantum Tunneling to Classical Hopping

A. J. Moreno, A. Alegría, and J. Colmenero*

Departamento de Física de Materiales y Centro Mixto CSIC-UPV/EHU, Universidad del País Vasco (UPV/EHU), Apartado 1072, 20080 San Sebastián, Spain

B. Frick

Institute Laue Langevin, BP 156X, F-38042 Grenoble, France

Received January 16, 2001; Revised Manuscript Received April 12, 2001

ABSTRACT: We present an extensive neutron scattering study on the ester methyl dynamics of poly(methyl methacrylate) (PMMA) in the temperature range from 1 to 200 K. The crossover from quantum tunneling to classical hopping has been investigated in an energy window from 0.5 μeV to 2 meV. Inelastic measurements of the librational levels have been performed in the millielectronvolt range. The results have been analyzed in terms of a model that considers a Gaussian distribution of potential barriers for methyl group rotation. A 6-fold correction to the main 3-fold term of the potential has been added to get a good description of the librational peak. This distribution of mixed-symmetry barriers gives an excellent description of the spectra in the whole temperature range.

1. Introduction

Among the different dynamical processes that take place in polymers, methyl group rotation is perhaps the simplest one, since all the relevant interactions on the methyl group can be condensed in an effective one-dimensional single-particle potential.[1−3] At sufficiently low temperatures, the chain backbones are frozen and secondary relaxations become very slow. In this temperature range, the methyl group dynamics is the dominating process, due to their much lower rotational potential barriers.[4−9] The development of a consistent model for this dynamics has a great interest not only from a basic point of view but also from a practical one, since it provides a starting point for the understanding of the local dynamics of more complicated molecular groups, as those supposed to be related with the most relevant mechanical properties of polymers.

Neutron scattering is a powerful tool to study the single-particle movements of molecular groups containing hydrogen atoms, since a selective deuteration allows to stand out the scattering coming from a particular group of hydrogens—the incoherent scattering cross section is 80 barns (1 barn = 10^{-24} cm^2) for the proton while only 2 barns for the deuterium. Moreover, from the dependence of the elastic intensity with the momentum transfer, it is possible to obtain the elastic incoherent structure factor (EISF), which provides information about the geometry of the motion. The different features of methyl group dynamics lie, in the case of low and moderate barrier systems, in the energy window accessible by neutron scattering, and a large number of studies in molecular crystals by using this technique have been published in the literature over the past 25 years.[3]

In crystalline systems, a quantum picture of the methyl group as a rigid-rotor tunneling through the rotational potential is usually taken at very low temperature ($T \approx 1$ K). For sufficiently low potential barriers the tunneling frequency, $\hbar\omega_t$, can be directly observed by neutron scattering in the microelectronvolt range as two inelastic peaks (for neutron energy gain and loss). For higher barriers the tunneling frequency lies beneath the best instrumental resolution nowadays available (a few tenths of a microelectronvolt), and other techniques are required, NMR being the most usual one (see for example refs 10 and 11). At high temperature (typically above 50−70 K) a simple classical description based on thermally activated incoherent hopping over the potential barrier is valid. The corresponding hopping rate follows an Arrhenius law driven by the classical activation energy E_A, defined as the difference between the top of the barrier and the ground state. The neutron scattering spectrum shows a quasi-elastic component that can be described by a Lorentzian of half-width at half-maximum (hwhm) $\Gamma = 3/(2\tau)$, $1/\tau$ being the hopping rate.[1] Thus, the quasi-elastic line broadens with increasing temperature as

$$\Gamma = \Gamma_\infty \exp(-E_A/kT) \qquad (1)$$

Γ_∞ being a temperature-independent preexponential factor. These two pictures (quantum tunneling at very low temperature and classical hopping at high temperature) are well established in crystalline systems, but nowadays it is known that they cannot be applied to methyl group dynamics in glassy systems—and particularly in polymers[12,13]—without taking into account the effects of the disorder present in these systems.

Methyl group rotational tunneling features were also expected in glassy polymers, and they were searched for a long time. Some indirect indications of quantum effects at low temperatures were obtained in the past by different techniques, as mechanical relaxation[14] or NMR.[15] These indications were based on the observation of a drastic lowering of the activation energy of the Arrhenius law for the characteristic hopping rate when

* Corresponding author: Tel 34 943 015962; Fax 34 943 212236; e-mail wapcolej@sq.ehu.es.

10.1021/ma0100854 CCC: $20.00
Published on Web 05/31/2001

decreasing temperature. This effect is a universal characteristic of the crossover from classical hopping to quantum tunneling in a great variety of physical processes,[16] but no further quantitative explanation was given to these results. Concerning neutron scattering, methyl group tunneling peaks were never observed. This was, in part, due to the generally high values of the rotational barriers in polymers, which correspond to tunneling frequencies not accessible by neutron scattering. Only a few low-barrier polymers were candidate to show methyl group tunneling features in neutron scattering spectra, as poly(vinyl acetate) (PVAc) and poly(methyl methacrylate) (PMMA), as confirmed recently.[13,17,18] In these two polymers, instead of the two inelastic peaks typically observed in crystals, the spectra showed an apparently quasi-elastic component even at very low temperature. A recent model—rotation rate distribution model (RRDM)—previously introduced to analyze the high-temperature behavior of the spectra[9,12] (see below) explained this result in terms of the distribution of tunneling lines, $h(\hbar\omega_t)$, that follows from a distribution of potential barriers for methyl group rotation. This latter distribution has its physical origin in the disorder present in the glassy state. Thus, the different individual environments of each methyl group—contrary to a crystal, where all the methyl groups are equivalent by translational symmetry—are reflected in different individual rotational barriers. According to the RRDM, the usual single-particle model is valid for each individual methyl group, whose spectrum follows the usual behavior of the crystalline case. The total spectrum of the glass is obtained as the weighted superposition of the individual spectra. When the distribution of potential barriers has a high average barrier or is sufficiently broad, the maximum of the distribution of tunneling lines lies beneath the instrumental resolution, yielding the apparently quasi-elastic component mentioned above. A convincing proof of this interpretation has been given by exploiting the well-known isotope effect on the tunneling frequency: deuteration of the methyl group yields a moment of inertia 2 times higher than that of the protonated one, resulting in a drastic reduction of $\hbar\omega_t$ (several orders of magnitude).[1−3] The isotope effect has been tested in PMMA, where the whole quasi-elastic-like feature hides beneath the instrumental resolution after deuteration of the methyl group.[17] Another proof has been obtained from measurements in low molecular weight glasses. In these systems, contrary to polymers, it is possible to make a direct comparison between methyl group dynamics in a same sample in crystalline and glassy state. The low-temperature spectra in the glass also show, as in the case of polymers, an apparently quasi-elastic component.[19,20]

The classical hopping picture at high temperature cannot be applied to glassy polymers in terms of a single hopping rate, as is usually done in the case of crystalline systems. Such a procedure yields the following unphysical results:[6,7,21] (i) a temperature dependence of the EISF, (ii) a non-Arrhenius dependence of the hopping rate, and (iii) a dependence of the obtained parameters on the energy window of the used spectrometer. These inconsistencies were removed when the RRDM was introduced.[9,12] In the framework of the model, the quasi-elastic Lorentzian characteristic for the single hopping rate of a crystal is now substituted by the distribution of Lorentzians following from the expected distribution of hopping rates. The hopping rate for each methyl group is driven by an Arrhenius-like law as eq 1 activated by its corresponding E_A.

Very recently, the RRDM has been extended to the whole temperature range incorporating the crossover regime between the tunneling and hopping limits, and it has been successfully checked on PVAc;[22] though in order to confirm the suitability of the extended version of the RRDM for the methyl group dynamics in glassy systems, it should be tested in more systems. The best candidate for a new test is perhaps PMMA, a material where methyl group dynamics has been exhaustively studied in the past.[4,6,7,17,23,24] It presents two families of methyl groups: one attached to the main chain (α-methyl) and another one in the ester group (ester methyl). The ester methyl is hindered by a barrier sufficiently low to yield observable effects in high-resolution neutron scattering even at very low temperatures, and moreover, in contrast to PVAc, it is possible to get selective deuterated samples.

In this work we present an extensive neutron scattering study of the ester methyl dynamics in PMMA up to 200 K in a wide dynamical range, and we show the suitability of the RRDM in the whole temperature range, covering the crossover from quantum tunneling to classical hopping limits. The paper is organized as follows: in section 2 we summarize the usual model for methyl group dynamics in crystalline systems as well as the nowadays well-established grounds of the RRDM in the tunneling and hopping limits. Then we show, on the basis of the knowledge about the crossover in crystalline systems, how to extend the RRDM to the whole temperature range. At the end of this section we present the neutron scattering functions derived in the framework of the RRDM. In section 3 we give experimental details. In section 4 we discuss the experimental results on PMMA in terms of the extended RRDM. Finally, conclusions are given in section 5.

2. Theoretical Aspects

a. The Crystalline Case. In the low-temperature picture of a rigid-rotor tunneling through a one-dimensional potential $V(\phi)$, the Hamiltonian is

$$H_R = -B(\partial^2/\partial\phi^2) + V(\phi) \qquad (2)$$

where $B = \hbar^2/2I$ is the rotational constant of the rigid rotor, I being the moment of inertia of the methyl group around its 3-fold symmetry axis. B takes a value of 7.6 K for a protonated methyl group. The potential is required to maintain the rotational symmetry of the methyl group. Therefore, it can be expanded as a Fourier series:

$$V(\phi) = \sum_{n=1}^{\infty} \frac{V_{3n}}{2}(1 - \cos(3n\phi + \delta_n)) \qquad (3)$$

In fact, it is straightforward to demonstrate that the rotor-lattice interaction can be expressed in this way by only supposing that it is given by a sum of two-body additive potentials.[25] In many systems it is sufficient to take only the 3-fold term $V_3(1 - \cos 3\phi)/2$ (see Figure 1), higher-order terms being, when needed, usually small.

The energy levels of the single wells are known as torsional or librational levels. The energies of the

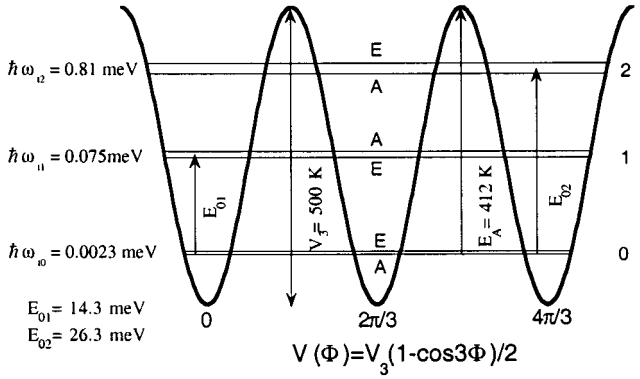

Figure 1. Level scheme for a pure 3-fold potential with barrier height $V_3 = 500$ K.

transitions between the ground and excited levels—we will refer to them as librational energies E_{0i}—lie in the millielectronvolt range and are strongly superposed with the phonon spectrum. This fact makes often difficult to distinguish in the neutron scattering spectra the librational transitions from frequencies corresponding to other modes.[26,27] By a selective deuteration it is possible to attenuate the scattering coming from modes not involving the motion of methyl group hydrogens, but not those different from librations that do involve it.

The coupling of the wave functions of the single wells splits the librational levels into the sublevels A and E, the latter consisting of the degenerate doublet (E_a, E_b). These sublevels have been labeled according to the irreducible representations of the symmetry group C_3 of H_R. The eigenstate A remains unchanged under a rotation $2\pi/3$, while such an operation adds a phase $\pm 2\pi/3$ to the spatial part of the wave functions of E_a and E_b, respectively. Thus, each eigenvector of H_R is characterized by two discrete quantum numbers: the librational number n and the symmetry index S (A, E_a, or E_b): $|nS\rangle$. At very low temperature only the ground librational level is appreciably populated, and the rotor oscillates coherently between the three wells with an oscillation frequency corresponding to the energy splitting between the ground sublevels A and E. For this reason, this frequency is usually known as the "tunneling frequency". The neutron scattering spectrum consists of a central elastic peak and two inelastic peaks centered at $\pm\hbar\omega_t$. The elastic peak results from both transitions without symmetry change and transitions $E_a \leftrightarrow E_b$. The inelastic peaks correspond to transitions $A \leftrightarrow E$.

It must be remarked that the tunneling frequency, librational energies, and classical activation energy are obtained as direct functions of V_3 by solving the Schrödinger equation for H_R. As an example, the level scheme for a barrier height $V_3 = 500$ K is shown in Figure 1.

When increasing temperature, the crossover from this quantum tunneling picture to the classical hopping regime takes place. From a large number of experiments[28−34] the phenomenology of the crossover in neutron scattering spectra of methyl group dynamics in crystalline systems is well established. Thus, the inelastic peaks broaden and shift toward the elastic peak. Moreover, a quasi-elastic component appears around the elastic peak. The quasi-elastic and inelastic lines can be well described by Lorentzian functions. It is also found that the hwhm's of these Lorentzians

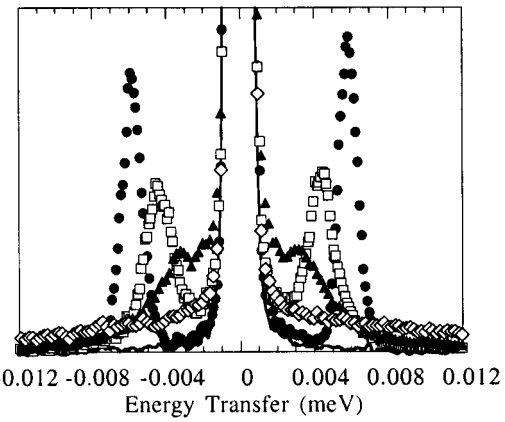

Figure 2. Methyl group dynamics in crystalline sodium acetate trihydrate: circles, rotational tunneling (2 K); squares and triangles, crossover regime (30 and 35 K, respectively); diamonds, classical hopping (50 K). The line is the resolution function.

follow Arrhenius laws activated by the first librational energy:[1−3]

$$\Gamma_{in} = \gamma_{in} \exp(-E_{01}/kT) \quad (4)$$

$$\Gamma_{qu} = \gamma_{qu} \exp(-E_{01}/kT) \quad (5)$$

The preexponential factor γ_{qu} of the Arrhenius law for the quasi-elastic Lorentzian is usually lower than that for the inelastic ones, γ_{in}, although they are of the same order of magnitude. The shift of the inelastic peaks also follows an Arrhenius law:[1−3]

$$\hbar\Delta\omega_t = \gamma_S \exp(-E_S/kT) \quad (6)$$

In this case the activation energy E_S is close to E_{01} but not necessarily equal. Finally, at higher temperatures, the quasi-elastic and inelastic lines merge in a central quasi-elastic line, reaching the classical hopping regime. The temperature where this merging occurs is not well-defined, though it takes place in a very narrow temperature range of the order of 7−10 K. In the following, we will refer to this somewhat ill-defined temperature as the "crossover temperature", T_C, that separates the quantum and classical regimes. Above T_C, the broadening of the quasi-elastic Lorentzian will follow an Arrhenius law driven by the classical activation energy (eq 1). This behavior is illustrated in Figure 2 in crystalline sodium acetate trihydrate.[35]

The problem of the crossover from rotational tunneling to classical hopping has raised great theoretical interest although nowadays a generally accepted model is still lacking.[36−47] The standard approach used to explain the features observed at least below T_C is that of the rigid rotor linearly coupled to a bath of harmonic oscillators, the latter representing the lattice phonons.[36,38,40−44,47] Thus, the Hamiltonian of the system is a sum of three terms: $H = H_R + H_B + H_C$. H_R is the rigid-rotor Hamiltonian in eq 2, H_B the Hamiltonian of the bath, and H_C the linear coupling between rotor and bath. The coupling is, as H_R, required to be invariant under the C_3 group. When coupling the rotor to the bath, the eigenvectors of H are now characterized by a large set of quantum numbers. However, since H is, as H_R, invariant under C_3, the symmetry index A, E_a, or E_b is again one of these quantum numbers. Thus,

the Dirac deltas of the low-temperature limit, corresponding to transitions between two eigenstates characterized by a symmetry index, are now substituted by Lorentzians, corresponding to transitions between two large sets of eigenstates, each set again characterized by a symmetry index, i.e.

$$|\xi S\rangle \rightarrow |\xi' S'\rangle$$

S and S' being the initial and final symmetry states and ξ and ξ' a large set of quantum numbers characterizing the initial and final state of the lattice. Within this picture, the inelastic Lorentzians involve transitions $A \leftrightarrow E$, while the quasi-elastic Lorentzian involves transitions $E_a \leftrightarrow E_b$. For this reason, we rewrite eqs 4 and 5 as

$$\Gamma_{AE} = \gamma_{AE} \exp(-E_{01}/kT) \tag{7}$$

$$\Gamma_{E_aE_b} = \gamma_{E_aE_b} \exp(-E_{01}/kT) \tag{8}$$

It can be seen that the elastic transitions without symmetry change do not lead to broadening,[41] yielding an elastic line as in the low-temperature limit. The calculation of the width and position of the Lorentzians is not a straightforward task, and it has no exact solution, so it has been tackled in different approximations.[36,38,40−44,47] All the calculations lead to the conclusion that the observed Arrhenius laws for the broadening and the shift are really the result of the sum over the Bose factors of the phonon frequencies of the bath. The weight for each Bose factor is a complicated expression involving the height of the barrier, the density of states, and the coupling constants of the rotor to the modes of the bath. For the broadening, the sum only involves the phonons resonant in librational levels. Thus, if the temperature is sufficiently low (in practice, for any temperature below T_C), the term resonant in the first librational level dominates and can be approximated as an apparent Arrhenius law driven by E_{01}. In the case of the shift, the sum involves the whole phonon spectra. However, the activation energy E_S of the apparent Arrhenius law results to be only slightly different from E_{01}.

b. Rotation Rate Distribution Model: Tunneling and Hopping Limits. Now we will see how the neutron scattering results for methyl group dynamics in glassy systems have been interpreted in the framework of the RRDM, i.e., by introducing a distribution of potential barriers $g(V_3)$ and assuming the usual crystal-like behavior for each individual methyl group. Because of the interdependence between the barrier height, the tunneling frequency, the librational energy, and the classical activation energy, $g(V_3)$ can be directly transformed into the corresponding distributions of these quantities:

$$g(V_3)\,dV_3 = f(E_A)\,dE_A = F(E_{01})\,dE_{01} = -h(\hbar\omega_t)\,d(\hbar\omega_t) \tag{9}$$

To get approximate numerical relationships between $\hbar\omega_t$, E_A, E_{01}, and V_3 that allow straightforward transformations, the Schrödinger equation for H_R was solved for a large range of V_3 values by using a standard diagonalization subroutine and a basis of 200 plane waves. For 70 K < V_3 < 2000 K the obtained relationships are

$$E_A(\mathrm{K}) = 0.940 V_3(\mathrm{K}) - 56.6 \tag{10}$$

$$E_{01}(\mathrm{meV}) = 1.42(V_3/B)^{0.549} \tag{11}$$

$$\hbar\omega_t = c\left(\frac{V_3/B}{d}\right)^{0.75} \exp\left[-\left(\frac{V_3/B}{d}\right)^{0.5}\right] \tag{12}$$

with $c = 2.58$ meV and $d = 0.580$.

As a first approximation the RRDM assumes a Gaussian distribution of purely 3-fold barriers. Up to now, the 3-fold approximation seems to be valid in all the systems analyzed in terms of the RRDM.[9,13,17−20,22,48] However, it is well-known that in some crystalline systems[3] it is necessary to include 6-fold corrections to the main 3-fold term in order to get the expected correspondence with the experimental values of $\hbar\omega_t$, E_A, and E_{01}. In principle, there is no reason to discard the possibility of 6-fold corrections in glassy polymers. Moreover, distributions alternative to the Gaussian shape could be found, especially for systems with an important population of nearly free rotors, where a Gaussian distribution requires a cutoff at zero energy. An example of these systems is glassy toluene.[20] In this case methyl group dynamics has been analyzed in terms of a more realistic Gamma distribution.

For the moment we will maintain the 3-fold approximation, and as polymers are high-barrier systems,[9,48] we will also assume a Gaussian shape for $g(V_3)$:

$$g(V_3) = \frac{1}{\sqrt{2\pi}\sigma_V} \exp\left(-\frac{(V_3 - V_{3o})^2}{2\sigma_V{}^2}\right) \tag{13}$$

Because of the linear dependence of E_A on V_3 (eq 10), the distribution $f(E_A)$ is also Gaussian:

$$f(E_A) = \frac{1}{\sqrt{2\pi}\sigma_E} \exp\left(-\frac{(E_A - E_{Ao})^2}{2\sigma_E^2}\right) \tag{14}$$

On the other hand, $F(E_{01})$ is slightly asymmetric (Figure 3a) while, due to the exponential dependence in eq 12, $h(\hbar\omega_t)$ turns to be extremely asymmetric. As mentioned above, the limited resolution of neutron scattering techniques can hinder the observation of the maximum of $h(\hbar\omega_t)$ and this distribution of tunneling lines can be reflected in the spectra as an apparently quasi-elastic component (Figure 3b). $F(E_{01})$ and $h(\hbar\omega_t)$ are shown in Figure 3 for an average barrier $V_{3o} = 800$ K and a half-width $\sigma_V = 250$ K, which are values typically obtained in polymers.[9,48]

In the high-temperature limit, each methyl group will perform classical hopping driven by its corresponding classical activation energy. In this way, the single quasi-elastic Lorentzian component of the crystalline case is substituted by a distribution of Lorentzians, each one following an Arrhenius-like temperature dependence as eq 1 or taking logarithms:

$$\log \Gamma = \log \Gamma_\infty - \frac{E_A \log(e)}{kT} \tag{15}$$

In principle, the preexponential factor Γ_∞ could depend on V_3. However, taking it as a barrier-independent quantity seems to be a good approximation.[12] By using

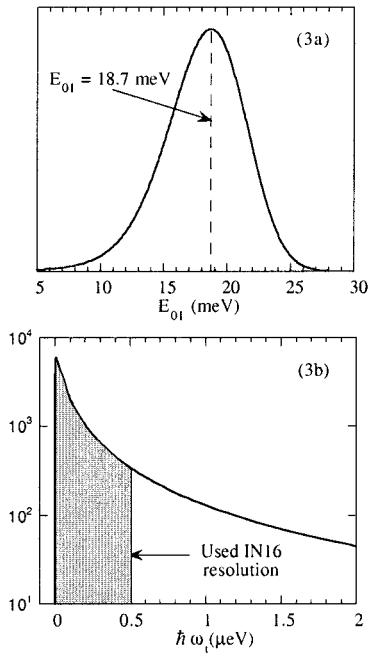

Figure 3. Distributions of first librational energies $F(E_{01})$ (a) and tunneling frequencies $h(\hbar\omega_t)$ (b) that follow from a Gaussian barrier distribution $g(V_3)$ with $V_{3o} = 800$ K and $\sigma_V = 250$ K. $h(\hbar\omega_t)$ is plotted on a logarithmic scale.

eqs 14 and 15, this latter approximation allows to transform the distribution of activation energies into a log-Gaussian distribution of hopping rates:[9,12]

$$H(\log\Gamma) = \frac{1}{\sqrt{2\pi}\sigma}\exp\left(-\frac{(\log\Gamma - \log\Gamma_o)^2}{2\sigma^2}\right) \quad (16)$$

with

$$\sigma = \sigma_E \log(e)/kT \quad (17)$$

From a least-squares fit of the spectra to a distribution of Lorentzians given by eq 16, a couple of values $\log\Gamma_o$ and σ are obtained at each temperature. Then, the values of Γ_∞ and E_{Ao} are determined from the fit of the average values $\log\Gamma_o$ to the Arrhenius law in eq 15. The value of σ_E can be obtained from fitting the values of σ to eq 17.

The distributions $h(\hbar\omega_t)$, $f(E_A)$, and $F(E_{01})$ can be determined respectively from low-temperature tunneling, high-temperature quasi-elastic and inelastic measurements. These distributions are obtained independently, but the consistency of the model requires that all of them can be transformed through eq 9 in the same $g(V_3)$. In this way, the only independent parameters of the RRDM are those characterizing $g(V_3)$, i.e., V_{3o} and σ_V, together with the preexponential factor for classical hopping Γ_∞.

c. Extension of the RRDM to the Crossover Regime. The evolution of neutron scattering spectra is more complicated to be interpreted in the case of a glass, due to the absence of defined peaks even at $T \approx 1$ K. In the framework of the RRDM, the spectrum of a glass is a superposition of crystal-like spectra weighted by $g(V_3)$, each individual spectrum evolving as described above: shift and broadening of the inelastic peaks and merging of the inelastic and quasi-elastic lines in a single quasi-elastic line when reaching T_C. According to the description given in section 2a, the evolution of each individual spectrum is controlled by different parameters: (i) the tunneling frequency, the first librational energy, and the classical activation energy (these three quantities depending directly on V_3); (ii) the preexponential factors for the different Arrhenius laws (in the case of Γ_∞, it can be taken as equal for every barrier as a good approximation); (iii) the crossover temperature where the merging of the three Lorentzians takes place.

We know that $g(V_3)$ and Γ_∞ can be obtained from the analysis in the low- and high-temperature limits. However, there is a large set of unknown parameters (namely for each barrier, the crossover temperature and the crossover preexponential factors) that cannot be obtained from a direct observation of the spectra, contrary to the crystalline case. Thus, the crossover temperature must, in principle, depend strongly on the height of the barrier, increasing for higher barriers. Moreover, the crossover preexponential factors depend on unknown coupling constants of the methyl group to the lattice phonons. In the crystalline case there is no need of knowing such constants to determine these factors, since these latter can be easily obtained from fits to the Arrhenius laws in eqs 6−8. However, this is not the case of the glass, where it is not possible to separate the individual shifts and broadenings.

Now we will see that all the above-mentioned problems can be removed by considering some reasonable approximations and introducing a definition of the crossover temperature for each barrier. Thus, we will assume that for a given methyl group, the classical behavior will be reached when the rate for incoherent hopping becomes comparable to the rate for coherent oscillations. Within this approach we define the crossover temperature as that where the condition $\Gamma/\hbar\omega_t = 1$ is satisfied, or, from eq 1,

$$kT_C = E_A/\ln(\Gamma_\infty/\hbar\omega_t) \quad (18)$$

Since E_A and $\hbar\omega_t$ are obtained as direct functions of V_3, for a given barrier the crossover temperature defined in this way depends only on its height V_3 and on the preexponential factor Γ_∞. This latter barrier-independent parameter can be understood as a measure of the strength of the coupling of the methyl groups to the lattice modes in a given system. For a given methyl group embedded in a system with a high value of Γ_∞; i.e., for a strong coupling, the classical regime will be reached at low temperature. Of course, eq 18 is a somewhat strict definition ("comparable" does not mean "equal", as required by this equation). However, it can be seen that changing the ratio $\Gamma/h\omega_t$ even by a factor of 2, T_C defined in this way does not vary beyond 5−10 K and therefore remains beneath the interval of experimental uncertainty where the merging of the three Lorentzians takes place.

In this way, when considering all the different methyl groups of the system, we have a new distribution, $G(T_C)$, that can be directly derived from $g(V_3)$ through eq 18. Figure 4 shows the corresponding distribution $G(T_C)$ for the previous example of Figure 3 with a typical value $\Gamma_\infty = 6$ meV.

Now we will make two new approximations for the temperature dependence of the broadening and the shift for each methyl group in the crossover range: (i) We will assume that the preexponential factors for the

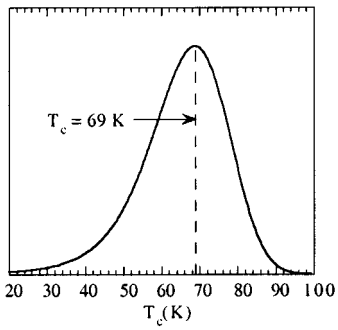

Figure 4. Distribution of crossover temperatures $G(T_c)$ corresponding to a barrier distribution distribution $g(V_3)$ with V_{3o} = 800 K and σ_V = 250 K and a value of 6 meV for the preexponential factor for classical hopping Γ_∞.

broadening of the quasi-elastic and inelastic Lorentzians are the same: $\gamma_{AE} = \gamma_{E_aE_b} = \gamma_b$, and therefore

$$\Gamma_{AE} = \Gamma_{E_aE_b} = \gamma_b \exp(-E_{01}/kT) \tag{19}$$

(ii) The activation energy for the shift will be taken exactly equal to E_{01}:

$$\hbar\Delta\omega_t = \gamma_S \exp(-E_{01}/kT) \tag{20}$$

As exposed above, we know from the phenomenology of the crystals that these two approximations are reasonable.

The set of eqs 1 and 18−20 describes the behavior of the spectra of each individual methyl group in the whole temperature range. In addition, we will impose two conditions to these equations at the crossover temperature.

(i) Continuity condition for the hwhm's of the Lorentzians: $\Gamma(T_C) = \Gamma_{AE}(T_C) = \Gamma_{E_aE_b}(T_C)$. Therefore, from eqs 1 and 19

$$\gamma_b = \Gamma_\infty \exp((E_{01} - E_A)/kT_C) \tag{21}$$

(ii) The tunneling frequency will be shifted to zero: $\hbar\Delta\omega_t = \hbar\omega_t$, as required by the disappearance of the inelastic processes at the classical onset. Thus, from eq 20

$$\gamma_S = \hbar\omega_t \exp(E_{01}/kT_C) \tag{22}$$

If the value of Γ_∞ is known, these two equations determine unambiguously the values γ_b and γ_S (actually $\gamma_b = \gamma_S$, from eqs 18, 21, and 22) for each barrier V_3, since $\hbar\omega_t$, E_{01}, and E_A are directly obtained as functions of V_3, and T_C defined as in eq 18 only depends on V_3 and Γ_∞. Therefore, the temperature evolution of each individual spectrum, given by eqs 1 and 18−20, is controlled only by two independent parameters: V_3 and Γ_∞. As an example, we illustrate in Figure 5 the temperature dependence of the shift and the different broadenings according to the above approximations for the typical values V_3 = 500 K and Γ_∞ = 6 meV.

In this section we have extended the RRDM to the whole temperature without adding new parameters to those already present in the low- and high-temperature limits, i.e., V_3, σ_V, and Γ_∞. Now we see how to derive, on the grounds of the RRDM, the neutron scattering functions for methyl group dynamics in glassy systems, following from the well-known functions for the three regimes in crystalline systems.

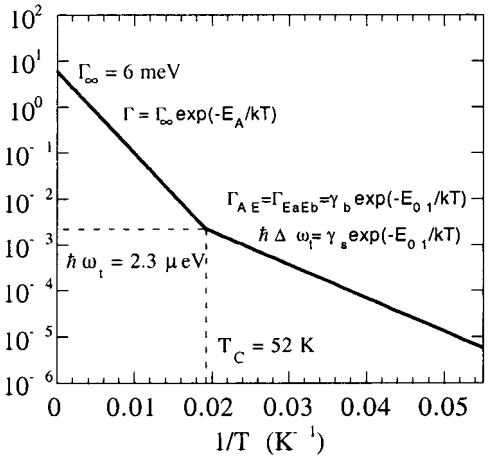

Figure 5. Temperature dependence of the shift and Lorentzian broadenings according to the approximations of the RRDM for a barrier height V_3 = 500 K and a preexponential factor Γ_∞ = 6 meV. The vertical axis is in meV units.

d. Neutron Scattering Functions. The incoherent scattering functions for each regime in the crystalline case are[1,28,44]

(i) tunneling regime:

$$S^{inc}_{MG}(Q,\omega) = \frac{5 + 4j_0(Qr)}{9}\delta(\omega) + \frac{2(1 - j_0(Qr))}{9}[\delta(\omega + \omega_t) + \delta(\omega - \omega_t)] \tag{23}$$

(ii) crossover regime:

$$S^{inc}_{MG}(Q,\omega) = \frac{1 + 2j_0(Qr)}{3}\delta(\omega) + \frac{2(1 - j_0(Qr))}{9}[L(\omega;\Gamma_{E_aE_b}) + L(\omega + (\omega_t - \Delta\omega_t); \Gamma_{AE}) + L(\omega - (\omega_t - \Delta\omega_t); \Gamma_{AE})] \tag{24}$$

(iii) classical regime:

$$S^{inc}_{MG}(Q,\omega) = \frac{1 + 2j_0(Qr)}{3}\delta(\omega) + \frac{2(1 - j_0(Qr))}{3}L(\omega;\Gamma) \tag{25}$$

where $\hbar Q$ and $\hbar\omega$ are the momentum and energy transfer of the neutron, j_0 is the zeroth-order Bessel function, and r is the H−H distance in the methyl group (r = 1.78 Å). It is straightforward to see that eq 24 reduces to eqs 23 and 25 in the two temperature limits. At very low temperature, the shift will be zero, and the three Lorentzians will have zero width, recovering eq 23. On the other hand, above the crossover temperature, $\Delta\omega_t = \omega_t$, and substituting the crossover hwhm, Γ_{AE}, and $\Gamma_{E_aE_b}$ by the classical Γ, we recover eq 25. Thus, for each individual methyl group its incoherent scattering function will be defined as eq 24 or 25 below or above, respectively, its crossover temperature.

The total incoherent scattering function of the RRDM will be the superposition of the individual spectra:

$$S^{inc}_{RRDM}(Q,\omega) = \int dV_3\, g(V_3)\, S^{inc}_{MG}(Q,\omega,V_3;\Gamma_\infty) \tag{26}$$

where the dependence of the individual spectra on V_3 and Γ_∞ has been explicitly indicated. Both the total coherent contribution and the incoherent contribution

of the other atoms in the sample are assumed to be elastic. Thus, the total scattering function can be written as

$$S(Q,\omega) = (\sigma^{coh}S(Q) + \sigma^{inc} - \sigma^{inc}_{MG})\delta(\omega) + \sigma^{inc}_{MG}S^{inc}_{RRDM}(Q,\omega) \quad (27)$$

where $S(Q)$ is the coherent static intensity, σ^{coh} and σ^{inc} are the total coherent and incoherent cross sections of the sample, and σ^{inc}_{MG} is the incoherent cross section of the three hydrogens of the methyl group. Finally, $S(Q,\omega)$ is convoluted with the instrumental resolution $R(Q,\omega)$ in order to make a quantitative comparison with the experimental spectra.

3. Experimental Details

Neutron scattering measurements were carried out on a syndiotactic PMMA sample from Polymer Source Inc. with M_n = 26 800 and M_w = 27 600. The chemical formula of the repeating unit is

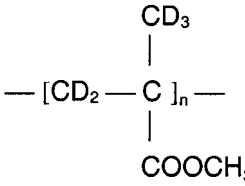

All the hydrogens except those of the ester methyl are substituted by deuteriums. The scattering cross sections of the monomer unit are σ^{coh} = 69.3, σ^{inc} = 250.9, and σ^{inc}_{MG} = 240.9 barns. A flat sample of thickness 0.75 mm was used to get a transmission close to 90%, avoiding multiple scattering effects in the Q range (1.3−1.9 Å^{-1}) we restricted to.

The backscattering and time-of-flight techniques were used in the spectrometers IN16 and IN6, respectively, at the Institute Laue Langevin (ILL, Grenoble, France). If ϕ and E_0 are respectively the scattering angle and the incident energy of the neutron, it is easy to get the relationship (see for example ref 49 or 50)

$$\frac{\hbar^2Q^2}{2m} = 2E_0 + \hbar\omega - 2\sqrt{E_0(E_0+\hbar\omega)}\cos\Phi \quad (28)$$

An incident wavelength λ_0 of 6.27 Å was used in IN16, yielding a Gaussian resolution with Lorentzian background. This resolution, of hwhm ≈ 0.4 μeV, was calibrated by a vanadium sample of thickness 1 mm. The measurements covered an energy window from −15 to 15 μeV and an angular range from 11° to 149°. As the maximum energy transfer is rather lower than the energy of the incident beam (2.1 meV), $\hbar\omega$ can be neglected in eq 28, which reduces to $Q = (4\pi/\lambda_0)\sin(\Phi/2)$, so constant angle will mean constant Q. The Q range obtained in this way goes from 0.2 to 1.9 Å^{-1}.

In the IN6 experiment a wavelength of 5.1 Å was selected, yielding a Gaussian resolution of hwhm ≈ 50 μeV, which was calibrated as in the IN16 experiment. The accessible angular range extended from 15° to 115°. Each angle covered an energy window typically from −2 to 1600 meV. In this case constant angle does not mean constant Q, and the scattering function $S(Q,\omega)$ was obtained by means of a standard interpolation program from the experimental $S(\Phi,\omega)$. We restricted the analysis to a Q and energy range from 0.4 to 2 Å^{-1} and from −2 to 2 meV, respectively.

The coherent contribution to the total scattering function of eq 27 was determined from a spin-polarization analysis on the D7 spectrometer at the ILL. The incident beam was vertically polarized, and the coherent static intensity $S(Q)$ was calculated from the measured spin-flip and non-spin-flip cross sections. $S(Q)$ for the studied sample is depicted in Figure 6.

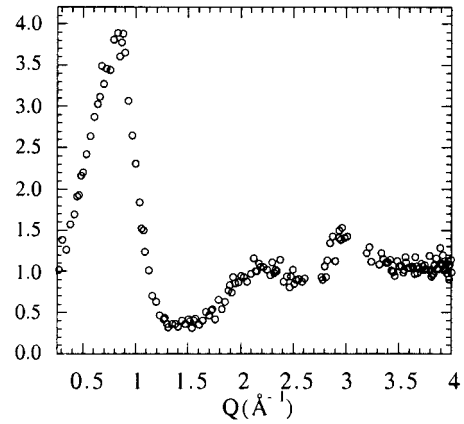

Figure 6. Coherent static intensity of the investigated PMMA sample.

Inelastic measurements were carried out in the time-of-flight spectrometer TOSCA at the ISIS pulsed spallation source at the Rutherford Appleton Laboratory (Chilton, UK). The TOSCA design is such that there is a unique value of Q for each value of the energy transfer, so all the detectors were summed up to obtain the vibrational spectrum.

4. Results and Discussion

Figures 7 and 8 show experimental spectra in IN16 and IN6 at different temperatures covering the rotational tunneling, crossover, and classical hopping regimes. As exposed in section 2, data were analyzed in terms of the convolution function $T(Q,\omega) = S(Q,\omega) \otimes R(Q,\omega)$, with $S(Q,\omega)$ given by eq 27. We started the analysis by a least-squares fit of the high-temperature spectra to the classical version of $T(Q,\omega)$. Thus, we took a superposition of classical-like functions as eq 25 weighted by a log-Gaussian distribution of hopping rates as eq 16 for the model function $S^{inc}_{RRDM}(Q,\omega)$. This latter function is the classical limit of eq 26, since $H(\log\Gamma)$ can be directly transformed into $f(E_A)$ and therefore into $g(V_3)$, as was exposed in section 2b. The temperature dependence of the parameters of the distribution $H(\log\Gamma)$ for classical hopping, $\log\Gamma_0$ and σ, is shown in Figures 9 and 10, together with the fits to eqs 1 and 17. Taking into account that low-energy vibrations are expected to contribute in the IN6 window, a flat background was introduced as additional parameter in the fitting procedure of the IN6 data. As required by any consistent model for methyl group rotation, the values of $\log\Gamma_0$ and σ at the common temperatures (160 and 200 K) for both instruments do not depend on the corresponding energy window.

The temperature dependence of the parameters of $H(\log\Gamma)$ are well described by eqs 1 and 17 above 80 K, but a clear deviation is found below this temperature, indicating the evidence of quantum effects. From the fit of the obtained set of values for σ to eq 17, a value σ_E = 241 K was obtained. The fits of the experimental spectra were redone, but now fixing the values of σ to those corresponding to σ_E = 241 K and leaving $\log\Gamma_0$ as the only fit parameter. This procedure only changes slightly the values of $\log\Gamma_0$ obtained in the fully free fit, yielding an average activation energy E_{Ao} = 710 K and a preexponential factor for classical hopping Γ_∞ = 4.8 meV. Solid lines in the spectra at 120, 160, and 200 K of Figures 7 and 8 show the theoretical $T(Q,\omega)$ functions in the classical limit, obtained by this latter fit with fixed σ_E.

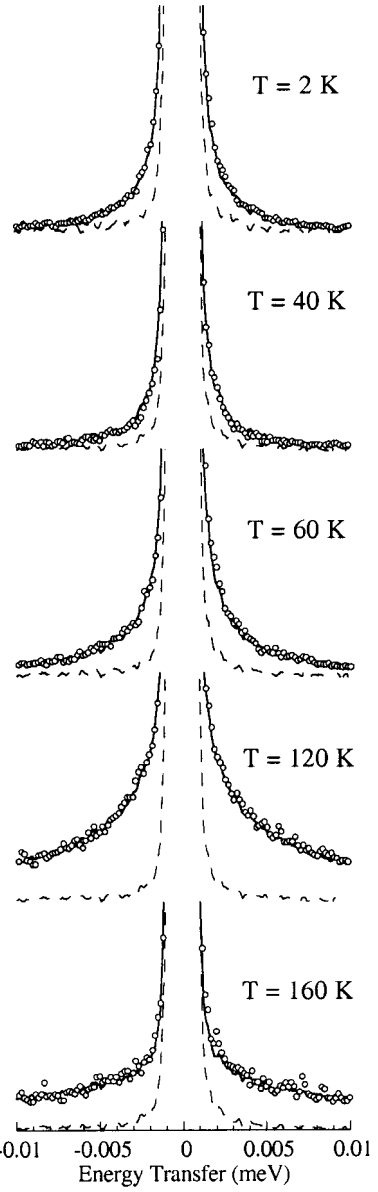

Figure 7. Experimental IN16 spectra at $Q = 1.8$ Å^{-1} for PMMA (points) and theoretical curves given by the RRDM (solid lines). The dashed line is the resolution function. The scale is a 5% of the maximum for all the plots.

The value obtained for the average activation energy is in close agreement with that of 638 K reported by Arrighi et al. in ref 6 and deduced from an analysis in the time domain based also on the idea of a distribution of hopping rates. In such an analysis, the time-exponential function, i.e., the Fourier transform of the Lorentzian, corresponding to the crystalline case is substituted in glassy systems by a Kohlrausch−Williams−Watt function. However, this latter analysis does not provide such a good agreement in its parameters when determined from measurements in different energy ranges,[9] the RRDM being a much better approach.

The distribution of classical activation energies given above transforms under the pure 3-fold assumption through eq 10 into a barrier distribution $g(V_3)$ with an average barrier $V_{3o} = 812$ K and half-width $\sigma_V = 255$ K. As it was reported in ref 17, the distribution of tunneling frequencies that follows from this $g(V_3)$ gives account for the low-temperature spectra (see the solid line in the spectrum at 2 K of Figure 7, corresponding

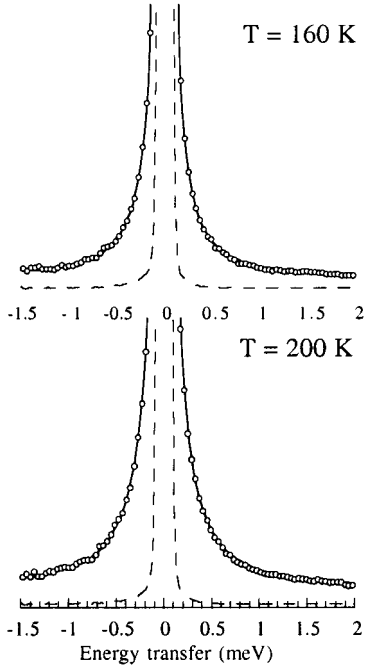

Figure 8. As Figure 6, for IN6 data. $Q = 1.6$ Å^{-1}.

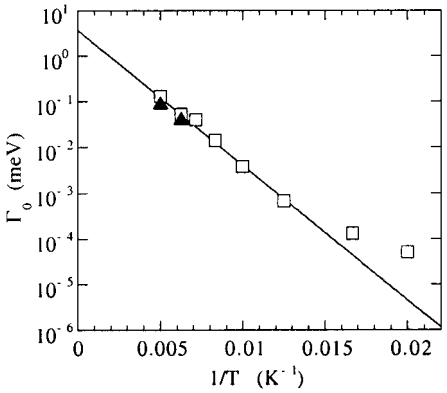

Figure 9. Temperature dependence of the Lorentzian hwhm for classical hopping corresponding to the average barrier: squares, IN16; triangles, IN6.

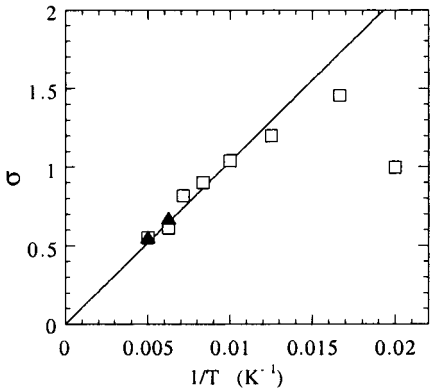

Figure 10. Temperature dependence of the half-width of the distribution $H(\log \Gamma)$ for classical hopping: squares, IN16; triangles, IN6.

to the theoretical $T(Q,\omega)$ in the tunneling limit). Therefore, the consistency of the RRDM in PMMA in the two temperature limits has been achieved.

To validate the so determined $g(V_3)$, we must check whether it is also able to account for the librational distribution $F(E_{01})$. To obtain information on such a

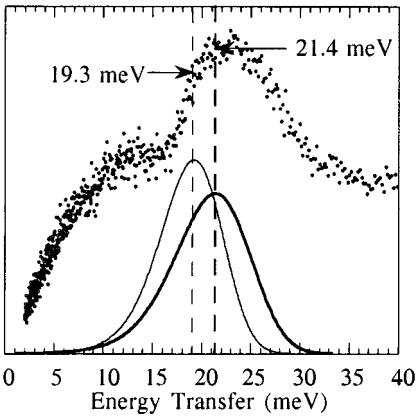

Figure 11. Experimental density of states (points) and librational distributions for a distribution of pure 3-fold barriers (thin line) and for mixed-symmetry barriers with $\eta = +0.11$ (thick line). The maxima of both distributions are indicated over the experimental data.

distribution, we carried out inelastic measurements in TOSCA. It is well-known from a large number of measurements in low- and moderate-barrier systems[28,29] that librational peaks are strongly damped with increasing temperature. Therefore, the measurements were taken at low temperature (20 K). Even at this temperature, $F(E_{01})$ cannot be well resolved from the experimental density of states due to the strong superposition of the librational modes with the phonon spectrum. Thus, our analysis was limited to the determination of the maximum of the librational peak, taking place about 22−23 meV (Figure 11). Despite the agreement of the early value reported in ref 4 with the present one, the former result was not sufficiently conclusive, since the measurements were taken at room temperature. The thin line in Figure 11 corresponds to the librational distribution $F(E_{01})$ that follows from the parameters of $g(V_3)$ given above. The maximum of such a distribution (19.3 meV) is clearly far from the experimental value at 22−23 meV. Given this inconsistency, we should reconsider the different assumptions of the model.

We remarked in section 2b that a Gaussian distribution of 3-fold barriers was a first approximation, but different kinds of distributions or higher-order Fourier terms should not be discarded. Thus, the analysis was redone in terms of a Gamma distribution $g(V_3)$ of pure 3-fold barriers:

$$g(V_3) = \left(\frac{\alpha}{e}\right)^{\alpha} \frac{1}{V_{3o}\Gamma(\alpha)} \left(\frac{V_3}{V_{3o}}\right)^{\alpha-1} \exp\left[-\alpha\left(\frac{V_3}{V_{3o}} - 1\right)\right] \quad (29)$$

with $\Gamma(\alpha)$ the Euler Gamma function and $\alpha \geq 1$. This asymmetric distribution reduces to an exponential when $\alpha = 1$ and to a Gaussian when $\alpha \to \infty$. A systematic increasing of the average barrier V_{3o} was obtained when decreasing the value of α. However, the increasing of V_{3o} (never further than 15%) was not sufficient to result in a significantly higher value for the librational peak, always remaining below 20 meV. Therefore, we can conclude that the characteristic values of the quantities relevant for methyl group dynamics (tunneling frequency, classical activation energy, or librational energies) in the glass do not depend critically on the shape of the distribution if this is sufficiently realistic. Therefore, in the following we will maintain the Gaussian approximation, and we will check the possibility of higher-order Fourier terms in the potential.

The inclusion of such terms raises a new problem, since, as the main 3-fold term, they can also be distributed, resulting in the introduction of additional parameters. To avoid this difficulty, as a first approximation we will introduce an in-phase 6-fold correction to the main 3-fold term:

$$V(\phi) = \frac{V_3}{2}(1 - \cos 3\phi) + \frac{V_6}{2}(1 - \cos 6\phi) \quad (30)$$

and we will impose a constant ratio $\eta = V_6/V_3$. Since the value of η is imposed beforehand (as in the pure 3-fold approximation, which takes $\eta = 0$), no new parameters are added to the RRDM. In this way the analysis procedure is exactly the same as in the pure 3-fold case. The only difference will lie in the relationships of eqs 10−12, which will be modified for the different values of η.

High-temperature neutron scattering measurements in PMMA of refs 6 and 7 reported an EISF corresponding to a classical 3-fold rotation, and posterior molecular dynamics simulations (MDS)[51] showed hopping of the three hydrogens between three equivalent positions. However, the introduction of a 6-fold correction must not be thought to be in conflict with these results, since in the classical regime, "3-fold" only means "hopping between three equivalent positions", but nothing is presupposed about the concrete functional form of the potential.[1,50] If the 6-fold term V_6 in eq 30 is sufficiently low (below 25% of V_3), it will yield a distortion of the cosine shape of $V(\Phi)$, but it will not result in extra potential minima (for $\eta < 0$) or maxima (for $\eta > 0$) and therefore will not affect the EISF. Since a pure 3-fold potential and another mixed-symmetry one can have the same E_A, and it is this quantity which controls the dynamics in the classical regime, high-temperature neutron scattering measurements or MDS will not be able by themselves to distinguish between both potentials. Only complementary measurements of the tunneling frequency and the librational energy can determine unambiguously the parameters of $V(\Phi)$. For example, a pure 3-fold potential with $V_3 = 400$ K and another one with $V_3 = 416$ K and $V_6 = 50$ K yield the same $E_A = 322$ K, though very different tunneling frequencies ($\hbar\omega_t = 6$ and 3.7 μeV, respectively) and librational energies ($E_{01} = 12.6$ and 14.5 meV).

Anyway, the results of refs 6, 7, and 51 indicate that 6-fold corrections in PMMA, if existing, are small, not resulting in additional potential maxima or minima. Thus, only corrections with $|\eta| < 0.25$ will be tried. As the distribution of activation energies obtained from our high-temperature analysis is independent of the possible existence of a 6-fold correction, the new distribution of mixed-symmetry barriers must be chosen so that it is still transformed in this $f(E_A)$. Moreover, we will retain the value 4.8 meV for the preexponential factor Γ_∞, since it has also been obtained from the classical analysis.

Concerning the tunneling and crossover regimes, the functional forms of eqs 23 and 24 will not be affected by the introduction of the 6-fold corrections. The weights of the Lorentzians and Dirac deltas appearing in such equations and corresponding to the pure 3-fold case are valid for moderate and high barriers, as is the case of PMMA, and for the range of momentum transfers accessible in the experiment ($Q < 2$ Å^{-1}).[52] In this case

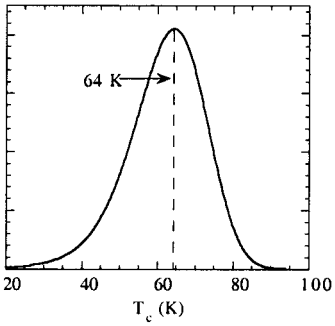

Figure 12. Distribution of crossover temperatures following from the obtained distribution of mixed-symmetry barriers.

the spatial part of the wave functions of the eigenstates A, E_a and E_b are well approximated as symmetry-adapted combinations of Dirac deltas localized in the three potential minima, so they will not be affected by the shape of the potential if $|\eta| < 0.25$, and therefore the amplitude transitions between such eigenstates will be the same as in the pure 3-fold case, yielding the same weights for the Dirac deltas and Lorentzians in eqs 23 and 24.

The best description of the librational peak within this new approach and maintaining a consistent description of the spectra in the tunneling and hopping limits was achieved for a ratio $\eta = +0.11$ and a distribution with an average barrier $V_{3o} = 820$ K and a half-width $\sigma_V = 265$ K—we remember that we retain the value $\Gamma_\infty = 4.8$ meV as the remaining parameter of the model. The new relationships equivalent to eqs 10−12 for $\eta = +0.11$ are

$$E_A(\mathrm{K}) = 0.914V_3(\mathrm{K}) - 54.4 \tag{31}$$

$$E_{01}(\mathrm{meV}) = 1.40(V_3/B)^{0.581} \tag{32}$$

$$\hbar\omega_t = c\left(\frac{V_3/B}{d}\right)^{0.75} \exp\left[-\left(\frac{V_3/B}{d}\right)^{0.5}\right] \tag{33}$$

with $c = 3.38$ meV and $d = 0.510$.

The corresponding distribution of librational energies $F(E_{01})$ obtained from the new parameters of the model through eq 32 is shown in Figure 11 (thick line). Within the 6-fold correction, a reasonable description of the librational maximum is achieved, improving notably that obtained in the pure 3-fold case. Curiously, this result retrieves an early suggestion—the possibility of a 6-fold component for the rotational barrier of the ester methyl in PMMA—that was pointed out from an analysis based in the old idea of a single rotational barrier.[4]

Once the parameters of the RRDM model for the ester methyl of PMMA have been well established, we have reached the point of checking the extension of the RRDM to the whole temperature range. As exposed in section 3c, such an extension does not require additional parameters. Figure 12 shows the distribution of crossover temperatures $G(T_C)$ obtained from the above parameters through eq 18. This figure evidences that the classical hopping regime dominates the methyl group dynamics above ca. 80 K, since the population of barriers with T_C higher than this temperature is negligible. Thus, it is below 80 K where the suitability of the extended RRDM to account for the quantum effects must be proved. (Above that temperature the extended RRDM reduces to its classical version.) Figure 7 shows the excellent agreement of the extended RRDM with the experimental data in the crossover range (spectra at 40 and 60 K).

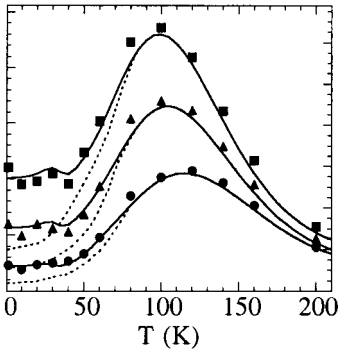

Figure 13. Integrated intensities in three inelastic windows: 1.5−5.6 μeV (squares), 2.5−6.5 μeV (triangles), and 5.6−10 μeV (circles). Solid lines are the theoretical curves given by the extended RRDM according to the distribution of mixed-symmetry barriers given in the text. Dotted lines correspond to a description exclusively in terms of classical hopping.

The temperature evolution of the spectra can be followed in more detail by depicting integrated intensities in different inelastic windows, as is shown in Figure 13, together with the theoretical curves predicted by the extended RRDM with the parameters given in this section. The description in terms of the classical model has been extrapolated to low temperature for comparison with experimental data. From this comparison, it is clear that the intensity excess over the classical curves due to quantum effects below about 80 K has been accounted for in the framework of the extended RRDM. Note that the agreement of the model with the experimental data in this region is not a result from a fitting procedure, but it is obtained from the parameters calculated from the analysis in the low- and high-temperature limits combined with the measurement of the librational peak.

5. Conclusions

By means of neutron scattering, we have checked the validity of the extended version of the RRDM—which connects the rotational tunneling and classical hopping regimes for methyl group rotation in glassy systems—in the ester methyl of PMMA. For this purpose we have combined two different spectrometers covering an energy range from 0.5 μeV to 2 meV. Moreover, we have carried out inelastic neutron scattering measurements of the density of states in order to obtain the librational peak. The consistency of the experimental peak maximum with that predicted by the RRDM with the parameters obtained from the analysis of the spectra in the low- and high-temperature limits requires a 6-fold correction V_6 to the main 3-fold term V_3 of the potential of each methyl group. A good agreement has been achieved in the simple approach of the same ratio V_6/V_3 for all the methyl groups. It is worthy of remark that the introduced 6-fold correction only means a slight distortion of the pure 3-fold potential, hardly modifying its shape.

Finally, by using the parameters obtained in the above procedure, the extended RRDM has been proved to give an excellent description of the experimental neutron scattering spectra in the whole temperature range, including the crossover region, without introducing additional parameters. The success of this analysis confirms this model as a suitable tool for the accurate

determination of the parameters of the barrier distribution for methyl group dynamics in disordered systems and particularly in glassy polymers.

Acknowledgment. The authors acknowledge Dr. J. J. del Val for the measurements of $S(Q)$ and Dr. D. Colognesi for experimental help in TOSCA. This work has been supported by the Spanish Ministry of Education (project PB97-0638), the Government of the Basque Country (Projects GV-PI98/20 and EX-1999/11), and the University of the Basque Country (Project 206.215-G20/98). The support of Donostia International Physics Center and Iberdrola S.A. is also acknowledged. A.J.M. acknowledges a grant of the Basque Government.

References and Notes

(1) Press, W. *Single Particle Rotations in Molecular Crystals*; Springer Tracts in Modern Physics Vol. 92; Springer: Berlin, 1981.
(2) Carlile, C. J.; Prager, M. *Int. J. Mod. Phys. B* **1993**, *7*, 3113.
(3) Prager, M.; Heidemann, A. *Chem. Rev.* **1997**, *97*, 2933.
(4) Gabrys, B.; Higgins, J. S.; Ma, K. T.; Roots, J. E. *Macromolecules* **1984**, *17*, 560.
(5) Frick, B.; Fetters, L. J. *Macromolecules* **1994**, *27*, 974.
(6) Arrighi, V.; Higgins, J. S. *Macromolecules* **1995**, *28*, 2745.
(7) Arrighi, V.; Higgins, J. S. *Physica B* **1996**, *226*, 1.
(8) Zorn, R.; Richter, D.; Frick, B.; Fetters, L. J., private communication.
(9) Mukhopadhyay, R.; Alegría, A.; Colmenero, J.; Frick, B. *Macromolecules* **1998**, *31*, 3985.
(10) Langen, H.; Montjoie, A. S.; Müller-Warmuth, W.; Stiller, H. *Z. Naturforsch. A* **1987**, *42*, 1266.
(11) van der Putten, D.; Diezemann, G.; Fujara, F.; Hartmann, K.; Sillescu, H. *J. Chem. Phys.* **1992**, *96*, 1748.
(12) Chahid, A.; Alegría, A.; Colmenero, J. *Macromolecules* **1994**, *27*, 3282.
(13) Colmenero, J.; Mukhopadhyay, R.; Alegría, A.; Frick, B. *Phys. Rev. Lett.* **1998**, *80*, 2350.
(14) Williams, J.; Eisenberg, A. *Macromolecules* **1978**, *11*, 700.
(15) Hoch, M. J. R.; Bovey, F. A.; Davis, D. D.; Douglas, D. C.; Falcone, D. R.; McCall, D. W.; Slichter, W. P. *Macromolecules* **1971**, *4*, 712.
(16) Benderskii, V. A.; Makarov, D.; Wight, C. A. *Chemical Dynamics at Low Temperatures;* Advances in Chemical Physics Vol. 88; John Wiley: New York, 1994.
(17) Moreno, A. J.; Alegría, A.; Colmenero, J.; Frick, B. *Phys. Rev. B* **1999**, *59*, 5983.
(18) Moreno, A. J.; Alegría, A.; Colmenero, J.; Mukhopadhyay, R.; Frick, B. *J. Non-Cryst. Solids*, in press.
(19) Moreno, A. J.; Alegría, A.; Colmenero, J.; Frick, B. *Physica B* **2000**, *276*−*278*, 361.
(20) Moreno, A. J.; Alegría, A.; Colmenero, J.; Prager, M.; Grimm, H.; Frick, B. ILL Exp. Rep 6-05-433, 2000.
(21) Chahid, A.; Colmenero, J.; Alegría, A. *Physica A* **1993**, *201*, 101.
(22) Moreno, A. J.; Alegría, A.; Colmenero, J. *Phys. Rev. B* **2001**, *63*, R60201.
(23) Higgins, J. S.; Allen, G.; Brier, P. N. *Polymer* **1972**, *13*, 157.
(24) Allen, G.; Wright, J.; Higgins, J. S. *Polymer* **1974**, *15*, 319.
(25) Emid, S. *Chem. Phys. Lett.* **1980**, *72*, 189.
(26) Clough, S.; Heidemann, A.; Paley, M. N. J.; Suck, J. B. *J. Phys. C* **1980**, *13*, 6599.
(27) Cavagnat, D.; Lascombe, J.; Lassegues, J. C.; Horsewill, A. J. *J. Phys. (Paris)* **1984**, *45*, 97.
(28) Prager, M.; Duprée, K. H.; Müller-Warmuth, W. *Z. Phys. B* **1983**, *51*, 309.
(29) Heidemann, A.; Prager, M.; Monkenbusch, M. *Z. Phys. B* **1989**, *76*, 77.
(30) Clough, S.; Heidemann, A.; Paley, M. N. J. *J. Phys. C* **1981**, *14*, 1001.
(31) Cockbain, J. R.; Lechner, R.; Owen, M.; Thomas, R. K.; White, J. W. *Mol. Phys.* **1982**, *45*, 1035.
(32) Cavagnat, D.; Magerl, A.; Vettier, C.; Clough, S. *J. Phys. C* **1986**, *19*, 6665.
(33) Prager, M.; Stanislawski, J.; Häusler, W. *J. Chem. Phys.* **1987**, *86*, 2563.
(34) Prager, M. *J. Chem. Phys.* **1988**, *89*, 1181.
(35) Moreno, A. J.; Alegría, A.; Colmenero, J.; Frick, B., to be submitted.
(36) Hüller, A. *Z. Phys. B* **1980**, *36*, 215.
(37) Clough, S.; Heidemann, A.; Horsewill, A. J.; Lewis, J. D.; Paley, M. N. J. *J. Phys. C* **1982**, *15*, 2495.
(38) Hewson, A. C. *J. Phys. C* **1982**, *15*, 3841, 3855.
(39) Clough, S.; McDonald, P. J.; Zelaya, F. O. *J. Phys. C* **1984**, *17*, 4413.
(40) Whittall, M. W. G.; Gehring, G. A. *J. Phys. C* **1987**, *20*, 1619.
(41) Würger, A. *Z. Phys. B* **1989**, *76*, 65.
(42) Hüller, A. *Z. Phys. B* **1990**, *78*, 125.
(43) Würger, A.; Hüller, A. *Z. Phys. B* **1990**, *78*, 479.
(44) Würger, A. *Z. Phys. B* **1991**, *84*, 263.
(45) Clough, S.; Horsewill, A. J.; Johnson, M. R. *Phys. Rev. A* **1993**, *47*, 3420.
(46) Clough, S.; Horsewill, A. J.; Johnson, M. R. *Chem. Phys. Lett.* **1993**, *208*, 143.
(47) Peternelj, J. *Phys. Rev. B* **1999**, *60*, 3989.
(48) Colmenero, J.; Moreno, A. J.; Alegría, A.; Álvarez, F.; Mukhopadhyay, R.; Frick, B. *Physica B* **2000**, *276*−*278*, 322.
(49) Lovesey, S. W. *Theory of Neutron Scattering from Condensed Matter*; International Series of Monographs of Physics; Clarendon Press: Oxford, U.K., 1984.
(50) Bée, M. *Quasielastic Neutron Scattering: Principles and Applications in Solid State Chemistry, Biology and Materials Science*; Adam Hilger: Bristol, U.K., 1988.
(51) Nicholson, T. M.; Davies, G. R. *Macromolecules* **1997**, *30*, 5501.
(52) Heidemann, A.; Anderson, I.; Jeffryes, B.; Alefeld, B. *Z. Phys. B* **1982**, *49*, 123.

MA0100854